Cellular/Molecular

Identification of Molluscan Nicotinic Acetylcholine Receptor (nAChR) Subunits Involved in Formation of Cation- and Anion-Selective nAChRs

Pim van Nierop,[1] Angelo Keramidas,[2] Sonia Bertrand,[2] Jan van Minnen,[1] Yvonne Gouwenberg,[1] Daniel Bertrand,[2] and August B. Smit[1]

[1]Department of Molecular and Cellular Neurobiology, Center for Neurogenomics and Cognitive Research, Faculty of Earth and Life Sciences, Vrije Universiteit, 1081 HV Amsterdam, The Netherlands, and [2]Department of Neuroscience, University Medical Centre, 1211 Geneva 4, Switzerland

Acetylcholine (ACh) is a neurotransmitter commonly found in all animal species. It was shown to mediate fast excitatory and inhibitory neurotransmission in the molluscan CNS. Since early intracellular recordings, it was shown that the receptors mediating these currents belong to the family of neuronal nicotinic acetylcholine receptors and that they can be distinguished on the basis of their pharmacology. We previously identified 12 *Lymnaea* cDNAs that were predicted to encode ion channel subunits of the family of the neuronal nicotinic acetylcholine receptors. These *Lymnaea* nAChRs can be subdivided in groups according to the residues supposedly contributing to the selectivity of ion conductance. Functional analysis in *Xenopus* oocytes revealed that two types of subunits with predicted distinct ion selectivities form homopentameric nicotinic ACh receptor (nAChR) subtypes conducting either cations or anions. Phylogenetic analysis of the nAChR gene sequences suggests that molluscan anionic nAChRs probably evolved from cationic ancestors through amino acid substitutions in the ion channel pore, a mechanism different from acetylcholine-gated channels in other invertebrates.

Key words: Lymnaea stagnalis; cholinergic receptor; ion selectivity; *Xenopus* oocyte expression; mutation; evolution

Introduction

Nicotinic acetylcholine receptors (nAChRs) belong to the Cys-loop family of ligand-gated ion channels (LGICs), which also include the 5-HT3 receptors (5-HT3Rs), $GABA_{A/C}$ receptors (GABARs), and glycine receptors (GlycRs), as well as the Zn^{2+}-activated receptor (Le Novere and Changeux, 1995; Ortells and Lunt, 1995; Davies et al., 2003). nAChRs are heteropentameric or homopentameric complexes of homologous subunits that each consist of an N-terminal extracellular ligand-binding domain (LBD) and four transmembrane domains that contribute to the formation of a channel pore. These receptors are typically divided in excitatory, cation-conducting nAChRs and 5-HT3Rs and inhibitory anion-conducting GABARs and GlycRs, which are also distinct with respect to ligand specificity. Experiments with chimeric constructs of Cys-loop superfamily subunits have shown that LBD and channel pore can be considered independent functional entities, because they can be exchanged between receptors while keeping intact the intrareceptor conformational change that couples ligand binding to ion channel opening (Eisele et al., 1993; Bouzat et al., 2004). The important sequence homology of the second transmembrane domain between cationic and anionic receptors of Cys-loop family further suggested that the ionic selectivity must be governed by a small group of residues that are lining the ionic pore. This hypothesis was confirmed by site-directed mutagenesis and the conversion of ionic selectivity of a cationic into an anionic channel (Galzi et al., 1992). These observations have, since then, been extended to different receptor subtypes, including the 5-HT3, $GABA_A$, and glycine receptors (Keramidas et al., 2000; Gunthorpe and Lummis, 2001; Jensen et al., 2002). In principle, the modular nature of ligand-gated ion channels, and the susceptibility to ion selectivity changes by limited mutations would predict the occurrence of naturally occurring recombination of ligand specificity and ion selectivity. Such events, however, do not seem to have occurred during mammalian evolution.

Molluscan species, however, are long known to display, in addition to excitatory, sodium-selective nAChRs, inhibitory chloride-selective nAChRs, suggesting that a natural recombination event of ligand specificity and ion selectivity has occurred during evolution of molluscan nAChRs (Tauc and Gerschenfeld, 1962; Vulfius et al., 1967, 2005; Kehoe, 1972a,b, 1976; Chemeris et al., 1982). Indeed, recently, acetylcholine-gated anionic channels have been characterized in *Caenorhabditis elegans* that are overall most similar to mammalian GABARs and GlycRs (Putrenko et al., 2004). These data suggest evolutionary adaptation of the ligand-binding site toward cholinergic ligands.

Here, we determined the nature of molluscan nAChRs to ac-

Received May 19, 2005; revised Sept. 29, 2005; accepted Oct. 3, 2005.

This work was supported by the Swiss National Science Foundation (D.B.). P.v.N. was supported by a grant from the Netherlands Organisation for Scientific Research, Technology Foundation STW.

Correspondence should be addressed to Dr. August B. Smit, Department of Molecular and Cellular Neurobiology, Center for Neurogenomics and Cognitive Research, Faculty of Earth and Life Sciences, Vrije Universiteit, De Boelelaan 1085, 1081 HV Amsterdam, The Netherlands. E-mail: guus.smit@falw.vu.nl.

A. Keramidas' present address: Department of Anesthesiology, Weill Medical College of Cornell University, New York, NY 10021.

DOI:10.1523/JNEUROSCI.2015-05.2005

 0270-6474/05/2510617-10$15.00/0

quire an understanding of evolutionary mechanisms behind the development of selectivity for either ligand binding or ion selectivity in the nAChR family. In this study, we selected subgroups of *Lymnaea* nAChR (LnAChR) subunits as putative anion- and cation-selective subunits based on amino acid sequences demonstrated previously to determine ion selectivity in mammalian nAChRs (Galzi et al., 1992). Functional expression of members of these subgroups in *Xenopus* oocytes revealed cation- and anion-selective channels. In contrast to the acetylcholine-gated channels in *C. elegans*, our data suggest that molluscan anion-selective nAChR subtypes have evolved from true cation-selective nAChRs by mutation of the ion channel pore.

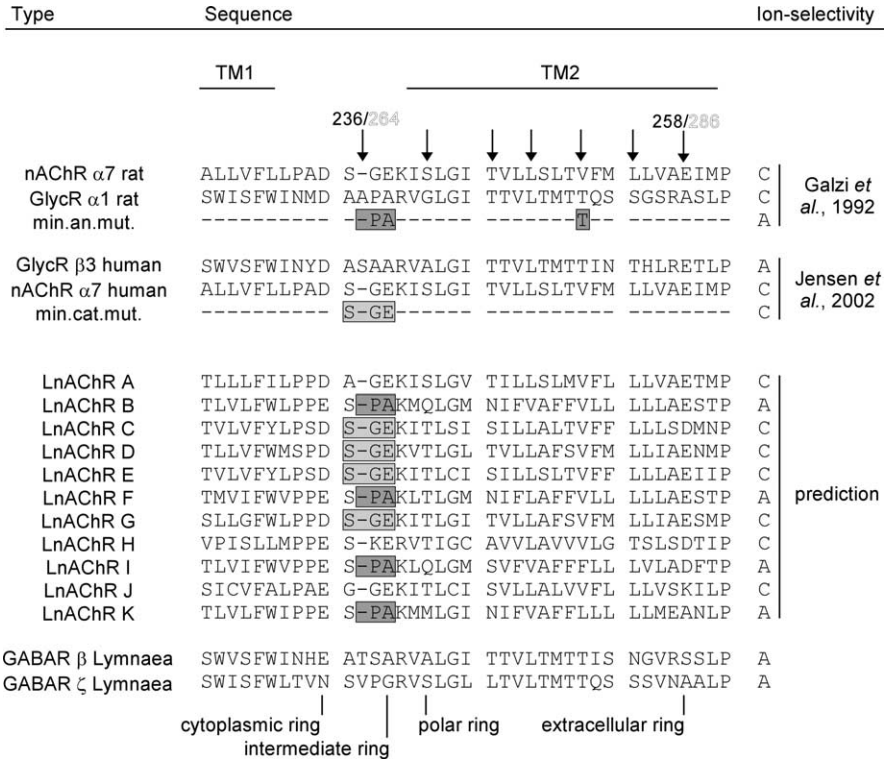

Figure 1. Putative anion selectivity-determining residues in LnAChR subunits. ClustalX alignment of the amino acid sequence around the TM1–TM2-joining loop of the LnAChR subunit proteins and corresponding regions of the cation-selective rat α7 nAChR subunit (GenBank accession number Q05941), the anion-selective α1 GlycR subunit (GenBank accession number CAC35978), the anion-selective human β3 GABAR subunit (GenBank accession number NP_068712) and the cation-selective α7 nAChR subunit (GenBank accession number P36544). Arrows indicate residues that are believed to face the lumen of the ion channel. The minimal anionic mutant (min.an.mut.) indicates rat α1 GlycR subunit-derived residues that are required and sufficient to induce anion selectivity in α7 nAChR subunit (Galzi et al., 1992). The minimal cationic mutant (min.cat.mut.) indicates rat α7 nAChR subunit-derived residues required and sufficient to induce cation selectivity in heteropentameric GABARs (Jensen et al., 2002). Indicated are residues similar to the minimal anionic mutant (dark gray boxes) and the minimal cationic mutant (light gray boxes). ***A***, ***C***, The presence and absence of corresponding motifs are used to predict anion (***A***) and cation (***C***) selectivity conferring properties of the LnAChR subunits. For comparison, corresponding regions of the anion-selective *Lymnaea* ζ GABAR subunit and β GABAR subunit are shown below. Residue positions that contribute to charged and polar rings in the channel pore that influence ion permeation are indicated (Jensen et al., 2002; Keramidas et al., 2004). Solid and outlined numbering corresponds to residues of the rat α7 nAChR subunit and LnAChR A, respectively.

Materials and Methods

Cloning of nAChR subunits. LnAChR subunits were identified as described previously (our unpublished observations). In short, PCR products representing partial coding sequences of nAChR subunit mRNAs were generated using nested combinations of degenerate oligonucleotides on a number of *Lymnaea* CNS-derived cDNA templates. Full-length sequences were obtained by a primer walking strategy on extended 5′ and 3′ sequences generated by PCR on a Lambda Zap II (Stratagene, La Jolla, CA) cDNA library of the CNS of *Lymnaea stagnalis*. Final sequences were obtained by sequencing three independently generated PCR products generated on dT-primed cDNA of pooled *Lymnaea* CNS. For *Xenopus* oocyte expression, cDNAs of open reading frames were cloned into pcDNA3 (Invitrogen, San Diego, CA). Sequences of cloned products were checked by dideoxy-chain termination sequencing. GenBank accession numbers of the sequences are as follows: LnAChR A, DQ167344; LnAChR B, DQ167345; LnAChR C, DQ167346; LnAChR D, DQ167347; LnAChR E, DQ167348; LnAChR F, DQ167349; LnAChR G, DQ167350; LnAChR H, DQ167351; LnAChR I, DQ167352; LnAChR J, DQ167354; LnAChR K, DQ167353; and LnAChR L, DQ167355.

Oocyte preparation. Xenopus laevis oocytes were prepared, injected, and recorded as described previously (Bertrand et al., 1990). Once isolated, each cell was intranuclearly injected with 2 ng of expression vector cDNA. Oocytes were then placed in 96-well microtiter plates (Nunc, Naperville, IL) at 18°C. Barth's solution used to store the oocytes consisted of 88 mM NaCl, 1 mM KCl, 2.4 mM $NaHCO_3$, 10 mM HEPES, 0.82 mM $MgSO_4$, 0.33 mM $Ca(NO_3)_2$, 0.41 mM $CaCl_2$, pH 7.4 adjusted with NaOH, and 100 U/ml penicillin.

Electrophysiology. Oocytes were used for experiments 2–4 d after cDNA injections. They were placed in the recess of a small chamber and continuously superfused with physiological medium. Solutions flowed at a rate of ~6 ml/min, and exchange was performed by the activation of computer-driven electromagnetic valves (type III; General Valve, Fairfield, NJ). Electrophysiological recordings were performed with a two-electrode voltage clamp (GeneClamp amplifier; Molecular Devices, Union City, CA). Electrodes were made out of borosilicate glass, pulled with a BB-CH-PC puller (Mecanex, Nyon, Switzerland), and filled with a filtered 3 M KCl solution. Oocyte Ringer's solution was used in control experiments as a bath solution [(in mM) 82.5 NaCl, 2.5 KCl, 5 HEPES, 2.5 $CaCl_2$, and 1 $MgCl_2$], pH 7.4, adjusted with NaOH.

The ion selectivity of homomeric LnAChR A or B channels was investigated using extracellular dilution potential experiments. The nAChR-mediated currents were elicited using a near-saturating concentration of acetylcholine (200 μM) dissolved in the appropriate extracellular solution. Current–voltage (*I–V*) relationships were recorded in control and three diluted extracellular solutions, in sequence, for each oocyte. The following extracellular solutions were used (in mM): control, 80 NaCl, 2.5 KCl, 0.2 $CaCl_2$, and 5 HEPES; test dilution 1, 40 NaCl, 2.5 KCl, 0.2 $CaCl_2$, 5 HEPES, and 74 sucrose; test dilution 2, 20 NaCl, 2.5 KCl, 0.2 $CaCl_2$, 5 HEPES, and 110 sucrose; test dilution 3, 20 NaCl, 2.5 KCl, 0.2 $CaCl_2$, 5 HEPES, and 127 sucrose (see Table 1). Sucrose was added to the diluted solutions to maintain osmolarity. The intracellular concentration of Na^+ (10.1 ± 0.7 mM), K^+ (109.5 ± 3.3 mM), and Cl^- (37.7 ± 1.2 mM) was taken from Costa et al. (1989). To minimize contamination by the endogenous calcium-activated chloride currents, all ion-selectivity experiments were performed in oocytes that had been incubated in BAPTA-AM (100 μM) for at least 5 h.

The current–voltage plots were fitted to polynomials and the reversal potentials were read directly from the plots. Liquid junction potentials were corrected using JPCalc software (Barry, 1994). The reversal-potential data were then pooled, and the averaged reversal potential (V_{rev}) was plotted against ion activity and fitted to the Goldman–Hodgkin–Katz (GHK) equation: $V_{rev} = (RT/F)\ln\{[P_{Na}\alpha_{Na}^{\circ} + P_K\alpha_K^{\circ} +$

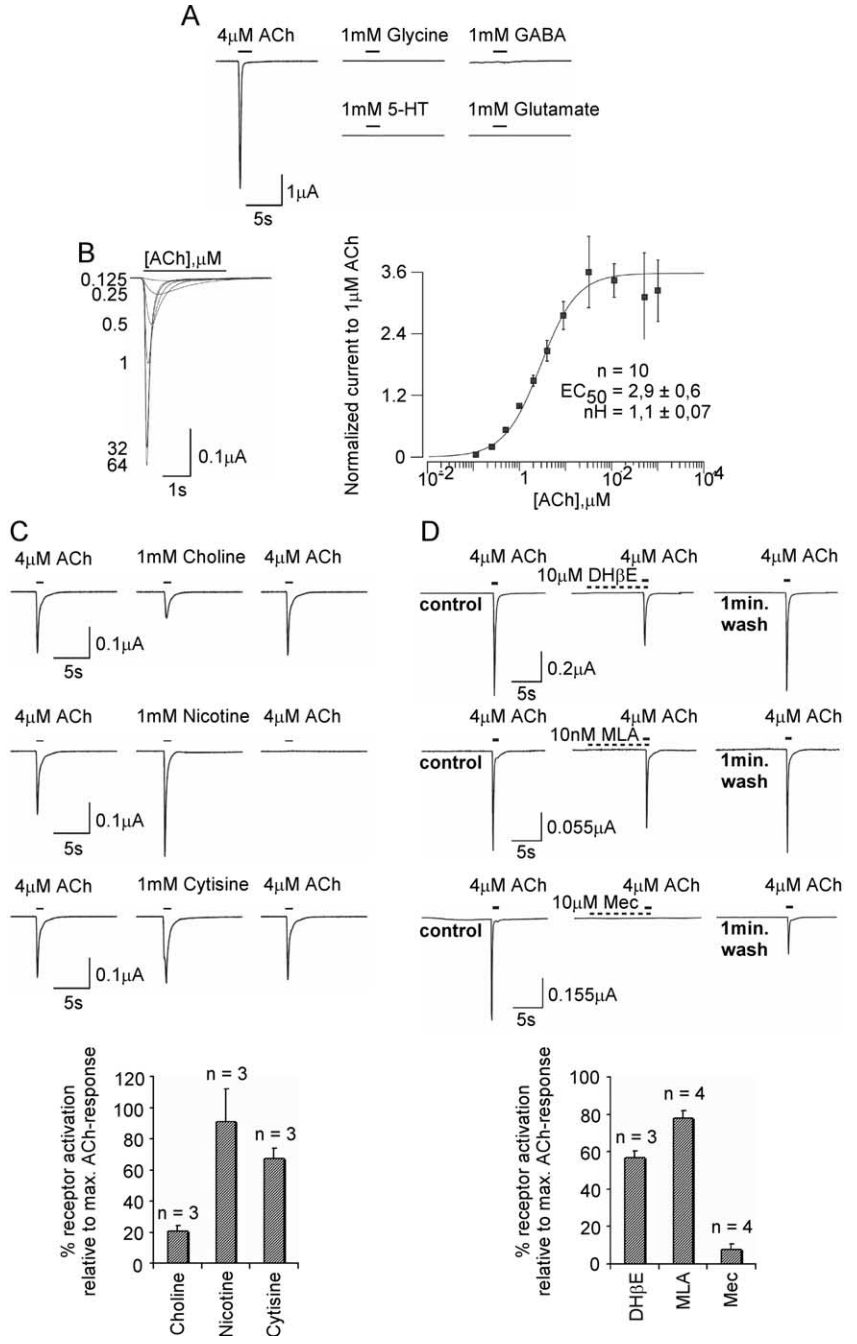

Figure 2. Sensitivity of the LnAChR A homopentameric receptor expressed in *Xenopus* oocytes to nicotinic drugs. The LnAChR A cDNA reconstitutes a homopentameric receptor in *Xenopus* oocytes. ***A***, Traces show currents elicited by pressure application of a low concentration of ACh and of high concentrations of glycine, GABA, 5-HT, and glutamate to oocytes expressing the LnAChR A subunit. Comparable results were observed on all oocytes tested (data not shown). ***B***, ACh-evoked currents were recorded using a range of ligand concentrations (0.1–1000 μM). A dose–response curve was inferred from ACh-induced mean peak current values normalized to the maximum and minimum values and indicates an EC_{50} value of ~3 μM. ***C***, The LnAChR A receptor is activated by the nicotinic agonists cytisine, choline, and nicotine. Before application of agonist, currents after a pulse of EC_{50} ACh was recorded to serve as a reference from oocytes expressing the LnAChR A subunit. The extent of desensitization resulting from agonist exposure was determined again by a pulse of ACh after a 1–3 min washout period. The graph reflects agonist-induced peak currents expressed proportionally to currents elicited by a saturating dose of ACh. ***D***, Sensitivity of LnAChR A receptors to DHβE, MLA, and Mec. The graph reflects the antagonist-induced reductions in peak current elicited by a saturating dose of ACh. max., Maximum. Error bars represent the SEM.

$P_{Cl}\alpha_{Cl}{}^{i}]/[P_{Na}\alpha_{Na}{}^{i} + P_{K}\alpha_{K}{}^{i} + P_{Cl}\alpha_{Cl}{}^{o}]\}$, where R is the Gas constant, T is temperature in Kelvin, F is Faraday's constant, P_{ion} is the permeability of the ion, and α_{ion} is the activity of the ion in the extracellular (superscript o) and intracellular (superscript i) solutions. All data are expressed as mean ± SEM.

All drugs, apart from α-bungarotoxin (αBtx) and α-conotoxin-ImI (αCtx-ImI), were applied by pressure application. α-Bungarotoxin (Sigma, Basel, Switzerland), α-conotoxin-ImI (American Peptide, Sunnyvale, CA), methyllycaconitine (MLA), dihydro-β-erythroidine hydrobromide (DHβE), mecamylamine (Mec) (Sigma) were diluted to the indicated concentration in the control medium that contained 20 μg/ml bovine serum albumin to prevent adsorption of the toxin on the plastics.

nAChR constructs. For expression in *Xenopus* oocytes, cDNAs representing open reading frames of LnAChR subunits were PCR amplified, separated on agarose gels, and cloned into *Bam*HI/*Xho*I-digested pcDNA3 (Invitrogen). Sequences of cloned products were checked by dideoxy-chain termination sequencing.

Phylogenetic analysis. Protein alignments were performed with ClustalX (Thompson et al., 1997). Phylogenetic analysis was performed using the neighbor-joining method (Kimura correction; gap positions included). Regions of weak alignment (corresponding to residues 1–24, 35–37, 188–192, and 324–452 of LnAChR A) were excluded from the analysis. Phylogenetic trees were midpoint rooted.

Real-time quantitative PCR. Total RNA was isolated from freshly dissected ganglia according to the method of Chomczynski and Sacchi (1987) using Trizol reagent (Invitrogen) that was followed by a DNase-I (10 U; Roche Diagnostics, Basel, Switzerland) treatment according to the instructions of the manufacturer, and a phenol/chloroform extraction and ethanol precipitation. cDNA was made using hexanucleotides (300 pmol) and 200 U of Moloney murine leukemia virus H– reverse transcriptase (Promega, Madison, WI). After cDNA synthesis, all samples were ethanol precipitated and dissolved in 60 μl of aquadest. Transcript-specific primers were designed using Primer Express software (Applied Biosystems, Foster City, CA): LnAChR A forward (fwd), 5′-gctaggaatgacctggaatgc-3′; LnAChR A reverse (rev), 5′-ggaacccacaccatctgctta-3′; LnAChR B fwd, 5′-tccagtttcgctacccagatg-3′; LnAChR B rev, 5′-gcgttggactcgacgatgt-3′; *Lymnaea* β-tubulin (Ltub) fwd, 5′-caagcgcatctctgagcagtt-3′; Ltub rev, 5′-tggattccgcctctgtgaa-3′. Primers were checked for specificity in GenBank by basic local alignment search tool analysis. PCR amplification efficiency of each primer set was determined by using a repetitive dilution series of total CNS cDNA; all primer sets showed an efficiency ≥1.9. Quantitative PCR (qPCR) measurements were performed using an ABI PRISM 7700 (Applied Biosystems) sequence detection system. PCR conditions and SYBR Green reagents (Applied Biosystems) were used in 20 μl reactions and with transcript-specific primers (300 nM) and 0.5 μl cDNA template according to the Applied Biosystems guidelines (40 cycles; 94°C for 30 s; 58°C for 30 s; 72°C for 210 s). After PCRs, temperature dissociation curves were generated to confirm the specificity of generated PCR products. The threshold line to determine the cycle of threshold (Ct value) was set on 0.3 ΔRn (baseline-subtracted values), with curves reaching maximally 6–8 ΔRn, and baselines of ~0.02 ΔRn. The obtained Ct values were used to calculate the relative level of gene expression (Ct_{norm}) normalized to Ltub (GenBank accession number X15542). For gene x the $Ct_{normgene x}$ is calculated by: $Ct_{gene x} - Ct_{Ltub}$. These values were transformed to yield

linear expression levels for each sample by the following: $2E - Ct_{normgenex}$. Then, relative gene expression levels of the transcripts from replicate measurements were calculated from normalized linear gene expression levels and expressed as mean ± SEM. With qPCR, the expression of all LnAChR subunits was detected in all CNS preparations with the highest Ct value (lowest abundance) measured at least six cycles (factor 32) from the Ct value of the no-template control.

In situ *hybridization. In situ* hybridization (ISH) was performed as described previously (Koert et al., 2001). Briefly, *Lymnaea* CNSs were frozen at −80°C, and 14 μm cryostat sections were mounted on SuperFrost slides (Menzel, Braunschweig, Germany). The sections were air dried and fixed in 1% paraformaldehyde and 1% acetic acid for 1 h. Sections were pretreated with 1.49% triethanolamine and 0.25% acetic acid, pH 8.0, and were passed through a graded series of alcohol (70–100%). Specific [^{32}P]UTP-labeled RNA probes were transcribed from linearized cDNA (200 ng) corresponding to stretches of coding sequence of LnAChR A (nucleotides 1039–1380) and B (nucleotides 1096–1470).

Results

Predicted ion selectivity of LnAChR subunits

In another work, we identified 12 neuronal nAChR (LnAChR) subunits from the freshwater snail *L. stagnalis* that possibly include subunits for cationic and anionic nAChR subtypes (our unpublished observations). The presence of a proline residue at the inner mouth of transmembrane domain 2 (TM2) is being thought of to determine anion selectivity, whereas the presence of a Ser-Gly-Glu motif at the corresponding position correlates to cation selectivity (Fig. 1) (Galzi et al., 1992; Keramidas et al., 2000; Gunthorpe and Lummis, 2001; Jensen et al., 2002). Of the identified LnAChR subunits, the LnAChR B, F, I, and K subunits possess proline residues in the TM1/TM2-joining loop, whereas LnAChR C, D, E, and G display the Ser-Gly-Glu residue motif. The LnAChR A, H, and J subunits all possess a Glu residue on a position corresponding to E237 (rat α7 nAChR), demonstrated be an important factor for cation selectivity (Keramidas et al., 2002; Wotring et al., 2003; Jensen et al., 2005b). Based on these findings, we predict, therefore, that LnAChR B, F, I, and K subunits participate in anion-selective nAChRs, whereas LnAChR A, C, D, E, G, H, and J participate in cation-selective nAChRs.

Functional expression of nAChRs composed of LnAChR A or LnAChR B

To determine the contribution of LnAChR subunits to functional receptors, we expressed LnAChR subunits in *X. laevis*

Table 1. Ionic composition of the solutions used for determination of the reversal potential

Estimated intracellular solution	Extracellular solutions			
	Control	Test dilution 1	Test dilution 2	Test dilution 3
$[Na^+]_i = 10.1 \pm 0.7$ mM[a]	$[Na^+]_o = 80$ mM (+ 2.0 mM Na^+ from NaOH)	$[Na^+]_o = 40$ mM (+ 2.0 mM Na^+ from NaOH) [sucrose] = 74 mM	$[Na^+]_o = 20$ mM (+ 2.0 mM Na^+ from NaOH) [sucrose] = 110 mM	$[Na^+]_o = 10$ mM (+ 2.0 mM Na^+ from NaOH) [sucrose] = 127 mM
$[K^+]_i = 109.5 \pm 3.3$ mM[a] $[Cl^-]_i = 37.7 \pm 1.2$ mM[a] $[Ca^{2+}]_i = 125.8 \pm 92.4$ nM[b] $[Mg^{2+}]_i > 0.5$ mM[b]	$[K^+]_o = 2.5$ mM $[Cl^-]_o = 82.9$ mM $[Ca^{2+}]_o = 0.2$ mM $[Mg^{2+}]_o = 0$ mM	$[K^+]_o = 2.5$ mM $[Cl^-]_o = 42.9$ mM $[Ca^{2+}]_o = 0.2$ mM $[Mg^{2+}]_o = 0$ mM	$[K^+]_o = 2.5$ mM $[Cl^-]_o = 22.9$ mM $[Ca^{2+}]_o = 0.2$ mM $[Mg^{2+}]_o = 0$ mM	$[K^+]_o = 2.5$ mM $[Cl^-]_o = 12.9$ mM $[Ca^{2+}]_o = 0.2$ mM $[Mg^{2+}]_o = 0$ mM

[a]From Costa et al. (1989).

[b]From Weber (1999).

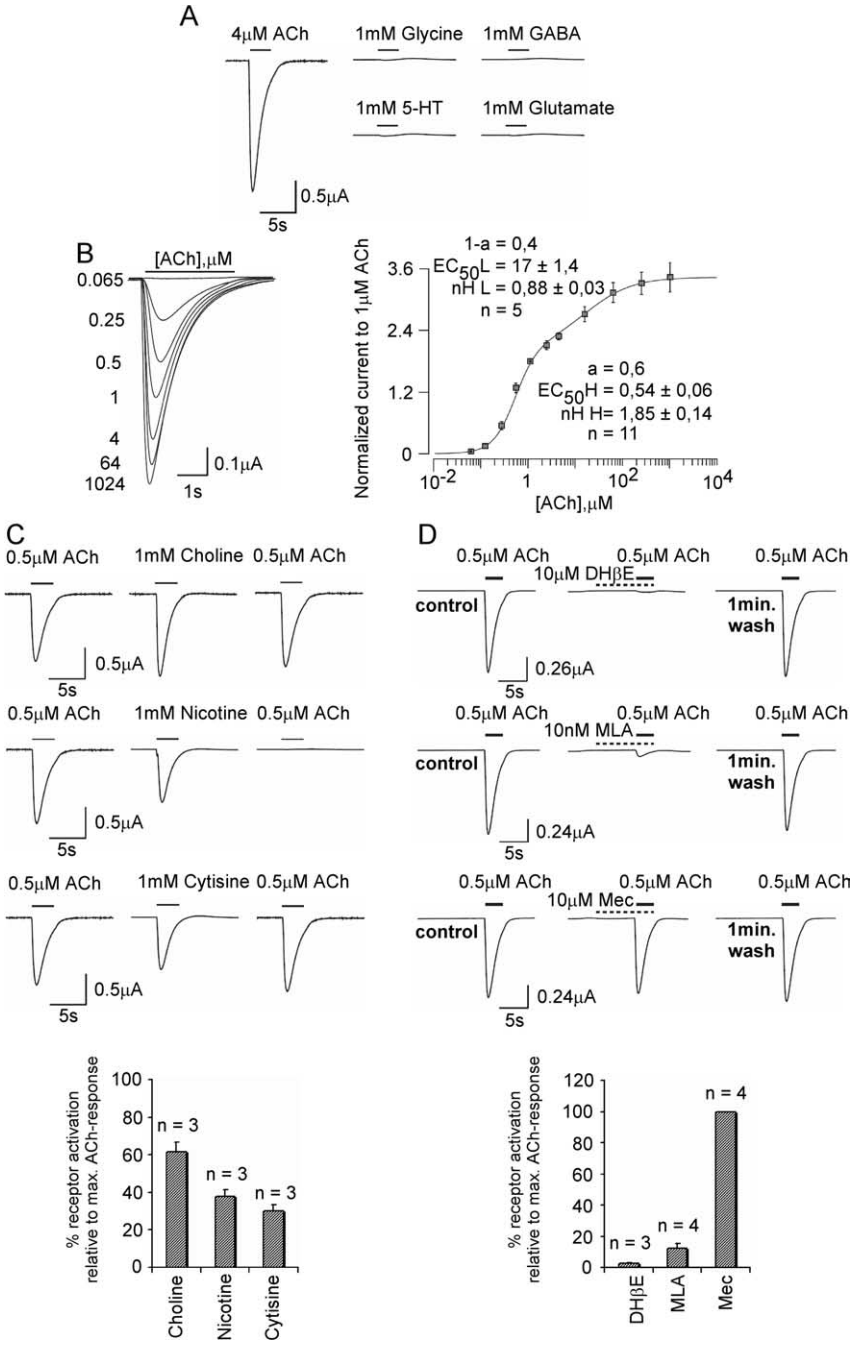

Figure 3. Sensitivity of the LnAChR B homopentameric receptor expressed in *Xenopus* oocytes to nicotinic drugs. ***A–D***, The analyses, as show in Figure 2, were applied to LnAChR B receptors expressed in *Xenopus* oocytes. ***B***, The dose–response curve of LnAChR B receptors for ACh reveals a biphasic pattern of binding, with the high-sensitivity component (H) of ~0.5 μM and a low-sensitivity component (L) of ~17 μM. max., Maximum. Error bars represent the SEM.

oocytes. As a first step, LnAChR subunits were expressed individually, allowing only homopentameric nAChR subtypes. Expression of functional receptors was observed with LnAChR A and B subunits.

The LnAChR A subunit is expressed as a rapidly desensitizing receptor that is activated by ACh (4 μM), but not by GABA, glycine, glutamate, or serotonin (Fig. 2*A*). This receptor displays an EC_{50} value of ~3 μM for ACh and a Hill coefficient of 1.1 (Fig. 2*B*). Determination of the pharmacological profile of this receptor revealed that, as is the case for the α7 receptor of vertebrates, a high concentration of choline (1 mM) is also able to activate the receptor (Fig. 2*C*). The typical nicotinic agonists nicotine and cytisine potently activate the LnAChR A receptor, the former inducing an irreversible state of desensitization (tested up to several minutes). ACh-evoked activation was partially blocked by a 10 μM concentration of the competitive inhibitor DHβE or the broad-spectrum noncompetitive inhibitor Mec (Fig. 2*D*). The selective blocker of vertebrate α7 nAChRs, MLA, yielded no specific inhibition of the ACh-evoked currents. Although insensitive to MLA, the LnAChR A receptor was markedly blocked by the competitive inhibitor αBtx, with properties resembling those of the vertebrate α7 receptors (see Fig. 4*A*). Moreover, the αCtx-ImI completely blocked receptor activation.

Expression of the LnAChR B yielded functional receptors that, as for LnAChR A, were activated by ACh but not by GABA, glycine, glutamate, or serotonin (Fig. 3*A*). The rate of desensitization of the LnAChR B receptor, however, is considerably lower than that of LnAChR A. Determination of the ACh dose–response curve revealed that LnAChR B receptors display a strongly biphasic sensitivity, as observed for the heteromeric $\alpha4\beta2$ receptors of vertebrates (Covernton and Connolly, 2000; Buisson and Bertrand, 2001). The high-affinity component is characterized by an EC_{50} value of 0.5 μM and a Hill coefficient of 0.88, whereas the low-affinity component has an EC_{50} value of 17 μM and a Hill coefficient of 1.5 (Fig. 3*B*). Determination of the pharmacological profile of the agonists revealed that, as for LnAChR A, these receptors can be activated by choline, cytisine, or nicotine (Fig. 3*C*). Interestingly, choline and nicotine are equipotent in activating the receptor. The LnAChR B receptor was fully blocked by the competitive nicotinic antagonist DHβE but not by the noncompetitive antagonist Mec (Fig. 3*D*). In contrast to the LnAChR A, both MLA (Fig. 3*D*) and αBtx (Fig. 4*B*) markedly inhibited the receptor, but only a small recovery from αBtx blockade could be observed after a 3 min wash, suggesting that this receptor is more sensitive to the snake toxin than the LnAChR A. In contrast, the LnAChR B receptors was insensitive to the αCtx-ImI (Fig. 4*B*).

Together, these data support classification of LnAChR A and B receptors as acetylcholine receptors of the nicotinic type, albeit with different pharmacological and biophysical characteristics.

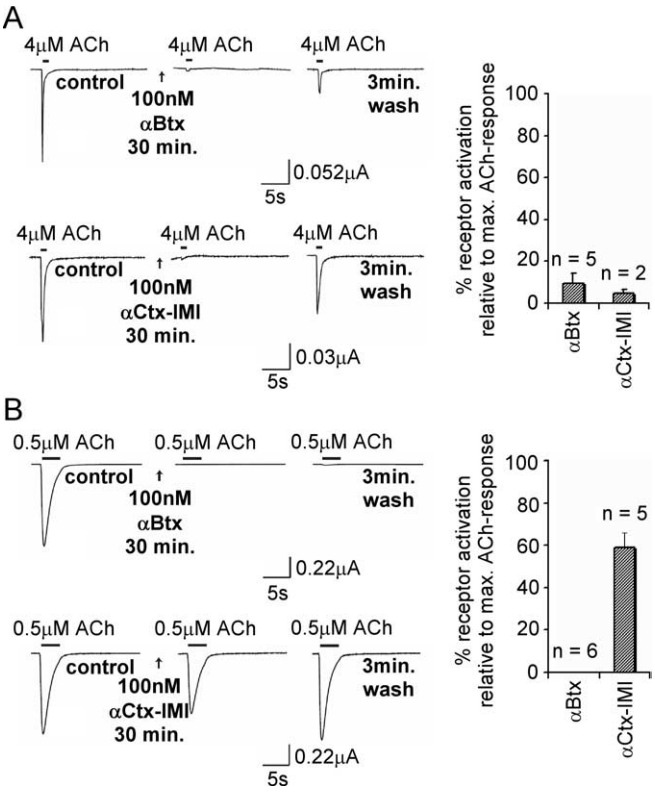

Figure 4. Sensitivity of the LnAChR A and LnAChR B homopentameric receptors expressed in *Xenopus* oocytes to protein toxins. Sensitivity of LnAChR A and LnAChR B receptors to αBtx and αCtx-ImI was tested. To compensate for differences in the diffusion rate, αBtx and αCtx-ImI were bath applied 30 min before ACh application. ***A***, With LnAChR A receptors, application of both toxins reduced ACh-induced currents to ~10% relative to control values (Table 1). ***B***, Application of αBtx completely abolishes ACh responses of LnAChR B receptors. αCtx-ImI displays much less potency with a maximal reduction of ~40% of ACh-induced responses. max., Maximum. Error bars represent SEM.

Ion selectivity of functionally expressed LnAChR A and B receptors

The successful reconstitution of LnAChR A and B receptors allowed determination of their ion selectivity. For this, *I–V* relationships were determined for LnAChR A and B receptors under different external ionic conditions. The ion charge selectivity of LnAChR A and B receptors was determined using dilution potential experiments. *I–V* relationships were recorded in a series of extracellular solutions in which Na^+ and Cl^- ions were diluted (see Materials and Methods). The experimental strategy was designed to reveal whether the channels preferred anions (Cl^-) or cations (Na^+ and K^+). The concentrations of potentially permeant divalent cations (Ca^{2+} and Mg^{2+}) were kept constant, as was the concentration of K^+. Examples of these experiments are shown in Figure 5 (left, LnAChR A; right, LnAChR B). For the LnAChR A channels, when extracellular NaCl is diluted, the reversal potential shifts in a leftward direction, toward the equilibrium potential for K^+ ($E_K = -92.1$ mV) (Fig. 5*A*,*B*). In dilution experiments, such as those illustrated by these results, the equilibrium potential for sodium ions progressively shifts toward zero, whereas the equilibrium potential for chloride shifts toward the right in the positive values. The leftward shift observed for the LnAChR A receptors indicate that this channel is mainly influenced by Na^+, making these channels predominantly cation selective. Plotting the reversal potential for all of the solutions tested versus the corresponding extracellular Na^+ concentration and fitting the data to the GHK equation yielded a chloride/sodium permeability ratio (P_{Cl}/P_{Na}) of 0.005 ± 0.001 (Fig. 5*C*). The best fit was achieved by fixing the potassium/sodium permeability ratio (P_K/P_{Na}) to 1.1. From our results, it can be inferred that the LnAChR A channels are ~200-fold more selective for cations over anions and exhibit no significant selectivity between Na^+ and K^+.

Similar experiments were performed on homomeric LnAChR B channels. In contrast to the LnAChR A channels, when extracellular NaCl was diluted, the reversal potential shifted in the direction of the equilibrium potential for Cl^- ions (Fig. 5*D*,*E*), suggesting predominantly anion-selective channels. Plotting the

reversal potential versus the extracellular Cl^- concentration and fitting the data to the GHK equation yielded a P_{Cl}/P_{Na} ratio of 111.4 ± 31.6 (Fig. 5*F*), showing an ~100-fold preference for anions over cations for these channels. These data confirmed the importance of the proline residue at the inner mouth of the channel domain, as predicted from the earlier ionic conversion performed by site-directed mutagenesis of the α7 nAChRs (Galzi et al., 1992; Corringer et al., 1999).

Phylogenetic analysis of LBD and ion channel domains of LnAChR subunits

Molluscan anion-selective nAChRs might have evolved along one of three distinct paths. The first is by mutation of the LBD of an anion-selective receptor (e.g., GABAR) that resulted in ACh sensitivity, similar to the acetylcholine-gated channels (Acc) of *C. elegans* (Putrenko et al., 2004). The second is by mutation of the ion channel of a cationic nAChR that resulted in anion selectivity. The third path is by recombination (e.g., by chromosomal crossover) of an nAChR LBD and a GABAR/GlycR ion channel, analogous to (*in vitro* constructed) chimeras of Cys-loop receptor subunits (Eisele et al., 1993; Bouzat et al., 2004). To distinguish between these three possibilities, we performed phylogenetic protein sequence comparisons for LBD and ion channel domains, separately (Fig. 6). This demonstrated that LBDs of all LnAChR subunits, including the group of the putative anion-selective LnAChR B, F, I, and K subunits, are most closely related to human nAChR/5-HT3R subunits. In line with this, also the ion channel domains are more closely related to corresponding domains of cation-selective as opposed to anion-selective receptor subunits, including known *Lymnaea* GABAR subunits (Bhandal et al., 1995). We conclude, therefore, that all domains of anion-selective LnAChR subunits are derived from a nAChR subunit ancestor, which implies that anion selectivity of *Lymnaea* nAChRs has evolved from within the nAChR subunit group by mutations leading to amino acid substitutions in the ion channel domain.

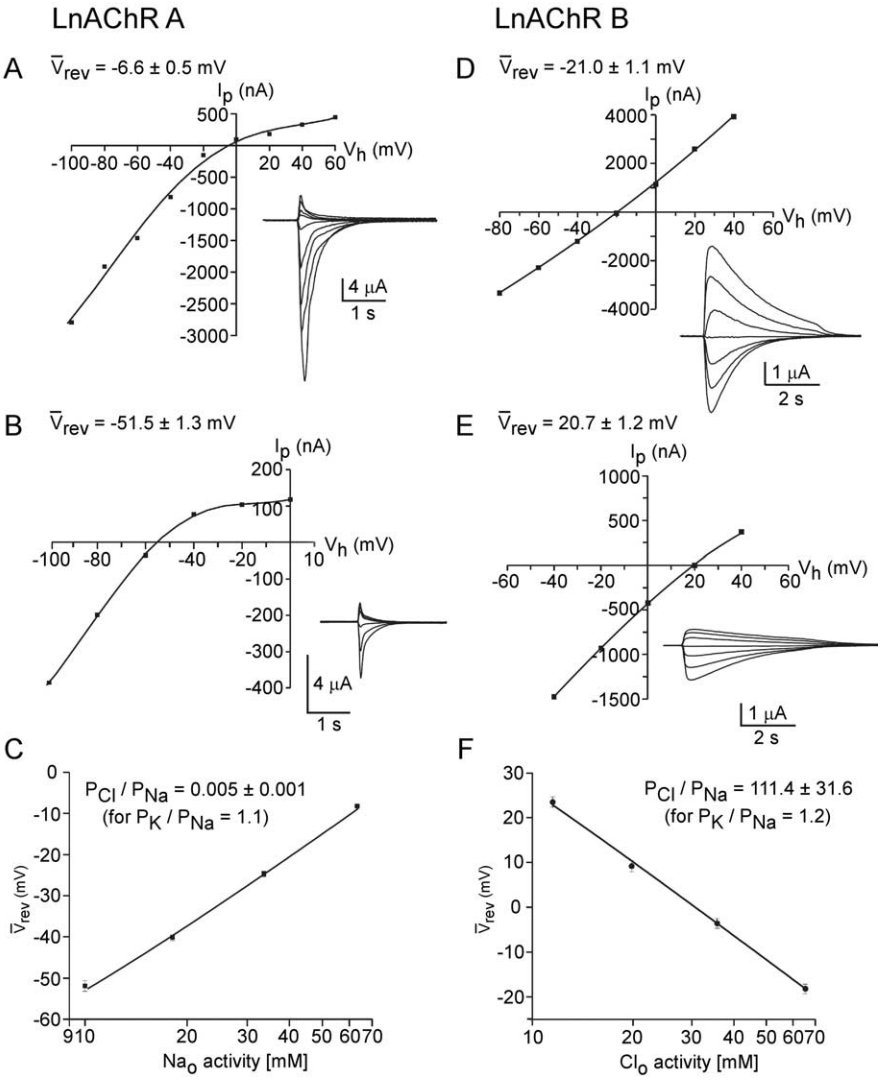

Figure 5. Ion selectivity of the LnAChR A and B homopentameric receptors expressed in *Xenopus* oocytes. ***A–C***, Determination of the effects of extracellular dilution of NaCl on the reversal potential of the LnAChR A receptors. ***A***, Current–voltage relationship of ACh-evoked currents were measured first in control solution. ACh-evoked currents (***A***, inset) were recorded at different holding potentials and the peak current was plotted as a function of the holding potential. The *I–V* data were fit with polynomial functions to estimate the reversal potential. The average reversal potential is shown for each *I–V* (V_{rev}, $n = 12$). ***B***, Reduction of NaCl concentration in the extracellular medium resulted in a significant shift in the reversal potential, measured as in ***A***, toward the predicted potassium equilibrium ($V_{rev} = -92.1 \pm 1.3$ mV; $n = 11$). ***C***, Plot of the reversal potential as a function of the logarithm of the extracellular sodium concentration and fit to the GHK equation (see Materials and Methods) yielded a P_{Cl}/P_{Na} value of 0.005 ± 0.001 for a $P_K/P_{Na} = 1.1$. ***D–F***, Determination of the ion selectivity of the LnAChR B receptors. ***D***, ***E***, Current–voltage relationships were measured using the same protocol as in ***A***, first in control conditions (***D***) and in a lower external NaCl concentration (***E***). Plot of the reversal potential as a function of the logarithm of the chloride concentration yielded a P_{Cl}/P_{Na} value of 111.4 ± 31.6 for a $P_K/P_{Na} = 1.2$ ($n = 11$). Error bars represent SEM.

Expression of LnAChR A and B subunits in the *Lymnaea* CNS

The expression of the LnAChR A and B, cationic and anionic receptors, respectively, in the central ring ganglia of the CNS was analyzed using real-time qPCR and ISH. qPCR showed that the LnAChR A subunit is most abundantly expressed in the cerebral ganglia, whereas lower levels of expression were detected in the pedal and buccal ganglia (Fig. 7*A*). ISH labeled few unidentified neurons in the cerebral, buccal and pedal ganglia, whereas little positive neurons were observed in other ganglia; the labeling intensity of the latter was considerably lower (Fig. 7*B*). In contrast to LnAChR A, the LnAChR B subunit is expressed at highest levels in the buccal ganglia and at lower levels in the pedal ganglia (Fig. 7*C*). This distribution was confirmed by ISH that showed clusters of labeled neurons in the buccal ganglia, as well as some labeled neurons in the pedal ganglia and sporadic positive neurons in the other ganglia (Fig. 7*D*).

Discussion

Based on molecular features of the TM1–TM2-joining loop demonstrated to influence ion selectivity, we defined groups within the identified family of LnAChR subunits presumed to participate in anion-selective (LnAChR B, F, I, and K) and cation-selective (LnAChR A, C, D, E, G, H, and J) nAChRs, respectively.

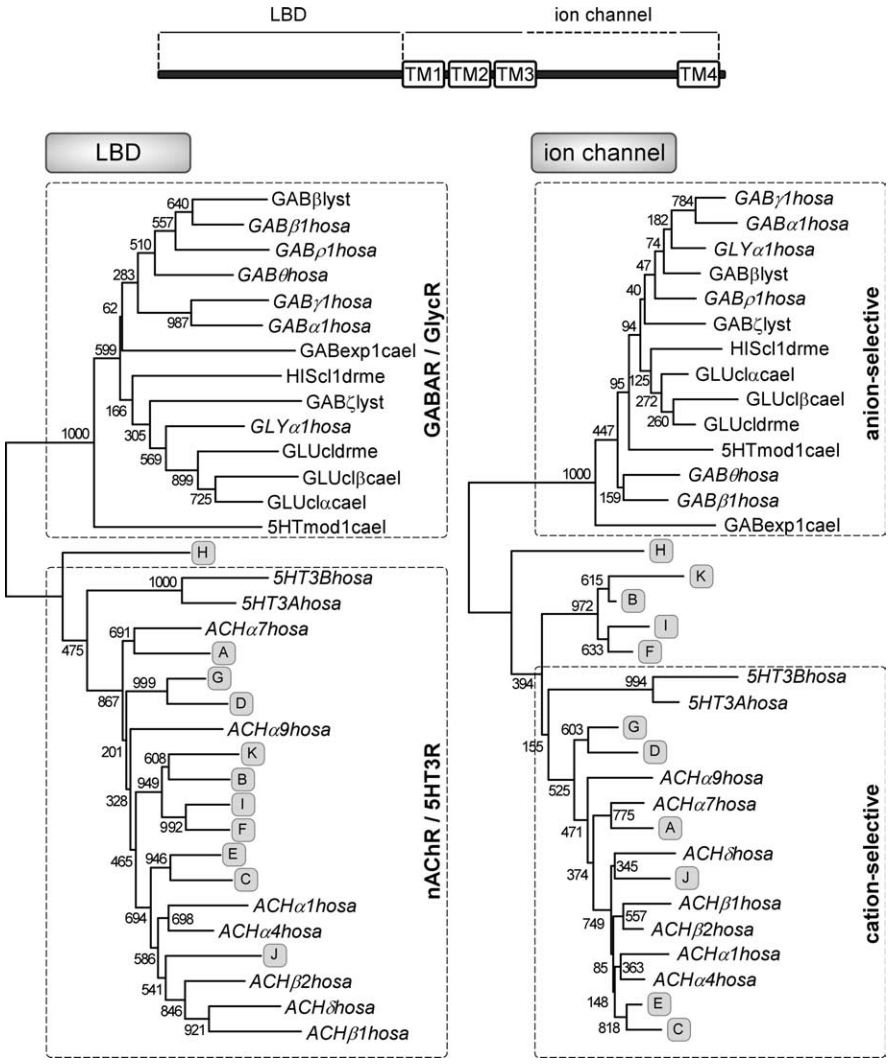

Figure 6. Sequence comparison of ligand-binding domains of LnAChR subunits and other members of the Cys-loop family of LGICs. ***A***, ***B***, LGICs phylogenetic comparison was performed on separate protein-sequence alignments of LBD (***A***) and ion channel (***B***) domains of invertebrate and human Cys-loop subunits. Indicated are transmitter phenotypes and ion selectivity of human subunits groups, respectively (dashed boxes). Human subunits are indicated in italics. ACH, Nicotinic acetylcholine receptor; GAB, GABA receptor A; GLY, glycine receptor, HIS, histamine receptor; cl, chloride channel; exp, EXP-1 gene product; mod1, MOD-1 gene product; ceal, *C. elegans*; drme, *D. melanogaster*; hosa, *Homo sapiens*; lyst, *L. stagnalis*. GenBank accession numbers for the sequences are as follows: 5HTmod1cael, N_741580; 5HT3Ahosa, AAH04453; 5HT3Bhosa, AAH46990; ACHα1hosa, NP_000070; ACHα2apca, AF467899; ACHα4hosa, NP_000735; ACHα7hosa, P36544; ACHα9hosa, NP_060051; ACHβ1hosa, NP_000738; ACHδhosa, NP_000742; GABα1hosa, NP_000797; GABβ1hosa, NP_000803; GABβlyst, X58638; GABexpcael, NP_495229; GABγ1hosa, NP_775807; GABρ1hosa, NP_002033; GABθhosa, NP_061028; GABζlyst, X71357; GLUclβcael, AAA50786; GLUcldrme, AAC47266; GLUclαcael, S50864; GLUclβcael, U14525; GLYα1hosa, AAH74980; HIScl1drme, AAL12210.

The validity of this prediction is supported by demonstrating the cation and anion selectivity of functionally expressed nAChRs composed of LnAChR A or B subunits, respectively. The definition of LnAChR B, F, I, and K as a presumed anion-selective subgroup is paralleled by a high overall sequence relatedness of these LnAChR subunits (our unpublished observations). Therefore, the LnAChR B, F, I, and K represent a group of related subunits that are constituents of anion-selective nAChRs.

In view of their pharmacological properties, the LnAChR A and LnAChR B receptors display similarities to the vertebrate α7 and α9 subunit-containing nAChRs. First, like α7 and α9 nAChRs, LnAChR A and B are functional homopentameric receptors when expressed in oocytes (Couturier et al., 1990; Elgoyhen et al., 1994; Gerzanich et al., 1994). Second, receptors composed of LnAChR A or B can be activated by choline, a weak but selective agonist of α7 and α9 homopentameric nAChRs (Papke et al., 1996; Alkondon et al., 1997; Verbitsky et al., 2000). Third, receptors composed of LnAChR A and B are sensitive to αBtx, a selective antagonist of α7- and α9-containing receptors in the vertebrate CNS (Schoepfer et al., 1990; Elgoyhen et al., 1994; Orr-Urtreger et al., 1997; Elgoyhen et al., 2001). Also, the LnAChR A receptor shows sensitivity to αCtx-ImI, and the LnAChR B receptor is selectively blocked by nanomolar concentrations of MLA, both properties that are attributed specifically to α7- and α9-containing nAChRs (Ward et al., 1990; Alkondon et al., 1992; Johnson et al., 1995; Palma et al., 1996). Pharmacological similarity of native molluscan nAChRs to vertebrate α7, α8, and α9 subunits has been noted in previous studies (Kehoe and McIntosh, 1998; Vulfius et al., 2005).

Unlike in the vertebrate nervous system, cholinergic transmission in the molluscan CNS is known to be mediated by cation- and anion-selective nAChRs (Tauc and Gerschenfeld, 1962; Vulfius et al., 1967; Kehoe, 1972a,b, 1976; Chemeris et al., 1982). Kehoe and McIntosh (1998) demonstrated the expression of two different anion-selective nAChR subtypes by identified cells in the buccal ganglia of *Aplysia*. In line with this, Vulfius et al. (2005) reported the expression of three distinct anion-selective nAChR subtypes by identified *Lymnaea* neurons. In addition, Woodin et al. (2002) showed, using whole-cell recordings on cultured *Lymnaea* soma–soma synapses, that, of the excitatory and inhibitory nAChR type(s) expressed by the right pedal dorsal 1 (RPeD1) neuron, the former can be selectively blocked by the cationic pore blocker Mec, which suggests the coexpression of cation- and anion-selective nAChRs by RPeD1. In addition to ion-selectivity differences of the channels, Woodin et al. (2002) described different properties of the ligand-binding sites of excitatory and inhibitory nAChRs expressed by RPeD1, as indicated by the distinct action of the competitive antagonists hexamethonium and MLA on excitatory and inhibitory nAChRs, respectively. In line with these data, the LnAChR A and B receptors display similar differential effects toward Mec and MLA application.

The LnAChR A and the LnAChR B subunits both display distinct patterns of expression characterized by a small number of expressing neurons in specific subsets of ganglia. The nonoverlapping expression pattern suggests that LnAChR A and B mediate each distinct task that is linked to a ganglion-specific function. For instance, in the buccal ganglia, a well characterized neuronal network involved in execution and regulation of feeding behavior resides (Benjamin and Elliott, 1989). Identified neurons of this

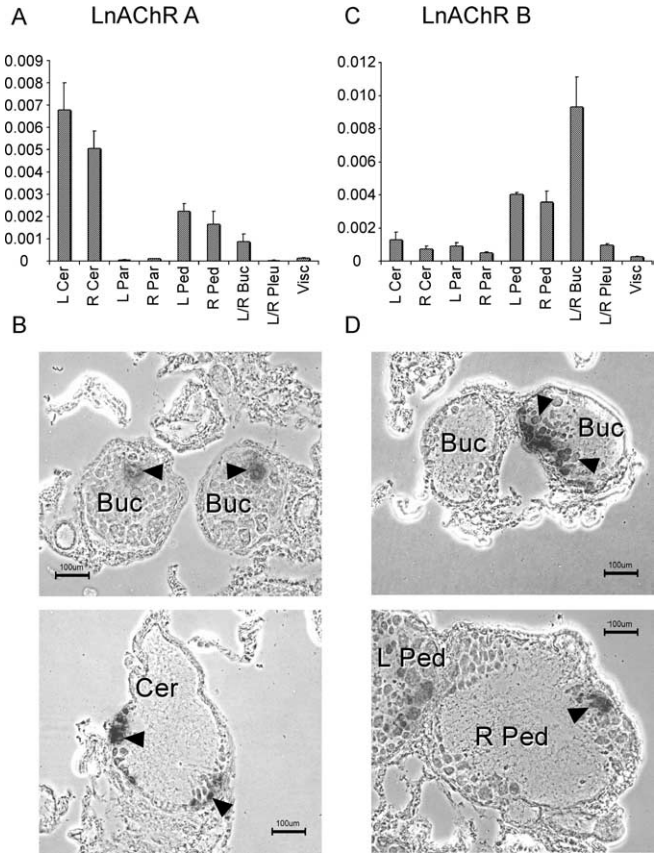

Figure 7. Expression of LnAChR A and LnAChR B transcripts in the *Lymnaea* CNS. ***A***, ***B***, Expression of LnAChR A (***A***) and LnAChR B (***B***) transcripts was measured by real-time quantitative PCR on cDNA preparations of independent pools of left and right buccal (L/R Buc; $n = 3$), left cerebral (L Cer; $n = 5$), right cerebral (R Cer; $n = 5$), left and right pleural (L/R Pleu; $n = 5$), left pedal (L Ped; $n = 4$), right pedal (R Ped; $n = 3$), left parietal (L Par; $n = 4$), right parietal (R Par; $n = 3$), and visceral (Visc; $n = 5$) ganglia. ***C***, ***D***, Expression levels were normalized to the expression of *Lymnaea* β-tubulin. Error bars represent SEM. *In situ* hybridization of LnAChR A (***C***) and LnAChR B (***D***) on the *Lymnaea* CNS. Shown for each subunit are examples of labeled neurons (arrowheads) at prominent sites of expression. Scale bars, 100 μm.

feeding network were shown to functionally express inhibitory nAChRs (Yeoman et al., 1993). The predominant expression of LnAChR B in the buccal ganglia matches this observation and justifies additional investigation into the involvement of LnAChR B in the feeding network.

Conversion of ion selectivity by molecular changes

In vitro mutagenesis studies (Galzi et al., 1992; Corringer et al., 1999; Gunthorpe and Lummis, 2001) suggested that anion selectivity is conferred by (1) insertion of a proline in the TM1–TM2-joining region, (2) substitution of Glu to Ala at position +1 relative to this proline (the intermediate charged ring), and (3) substitution of Val to Thr at position +15 (Fig. 1). Because anion-selective vertebrate LGICs and *Lymnaea* nAChRs have evolved along distinct evolutionary paths (for >600 million years), the convergent evolution of a proline positioned at the cytoplasmic border of TM2 supports the importance of this residue in establishing anion selectivity. However, the indifferent length of the TM1–TM2-joining region in anion-selective and cation-selective LnAChR subunits suggests that anion selectivity by itself does not require the insertion of the proline but that substitution is allowed as well. In addition, cationic LnAChR subunits contain negatively charged Glu residues in the intermediate ring (Jensen et al., 2002, 2005b; Keramidas et al., 2002), whereas anionic LnAChR subunits possess uncharged Ala residues (Galzi et al., 1992; Corringer et al., 1999; Gunthorpe and Lummis, 2001). Our data, therefore, confirm the importance of negatively charged residues in the intermediate ring for cation selectivity and the removal of these charges for anion selectivity, with Ala as the preferred substituent. Moreover, several charged or polar rings in the LGIC pore are known to influence ion permeation (Fig. 1), but mounting evidence suggests that discrimination between cations and anions is influenced by the intermediate charged ring (for review, see Keramidas et al., 2004; Jensen et al., 2005a). The similar residue properties of cation- and anion-selective LnAChR subunits in all but the intermediate ring support this notion. Last, none of the anion-selective LnAChR subunits show a Thr residue at position +15, indicating that other adaptive changes that mimic the Val-to-Thr substitution are allowed. Together, comparison of anion- and cation-selective LnAChR subunits suggests that presence of a proline residue in the TM1–TM2-joining region in combination with charge removal in the intermediate ring are preferred for the cationic-to-anionic conversion of LGICs.

Although our data are supportive of an important role of a proline residue insertion at the border of TM2 in determining anion selectivity, alternative molecular mechanisms might exist. For instance, in the chloride-conducting GABAR of $\beta3_2/\alpha2_2/\gamma2_1$ stoichiometry, only the $\alpha2$ and $\gamma2$ subunits possess prolines in the TM1–TM2-joining region, whereas $\beta3$ does not. Jensen et al. (2002) demonstrated that the ion selectivity of these heteropentameric GABARs can only be converted by introduction of the Ser-Gly-Glu motif of the TM1–TM2-joining region of the $\beta3$ subunit, demonstrating that cation selectivity can be induced despite the presence of prolines in $\alpha2$ and $\gamma2$ subunits. These findings hint at subunit-specific differences in dominance over ion selectivity, which might only become apparent in heteropentameric receptors.

Evolutionary perspective

A number of invertebrate species are known to express LGIC types that cross the ligand specificity/ion selectivity boundaries as present in vertebrates (Cully et al., 1994, 1996; Horoszok et al., 2001; Gisselmann et al., 2002; Beg and Jorgensen, 2003; Putrenko et al., 2004). Our findings show that anionic nAChRs in *L. stagnalis* represent true nAChRs that have acquired the ability to conduct anions by specific mutations in the ion channel domain. This is different from Acc 1 and Acc 2, found in *C. elegans* (Putrenko et al., 2004). These receptor subunits are highly similar to vertebrate GABA or glycine receptor subunits and lack the characteristic conserved residues of the ligand-binding site of nAChRs. As such, the *C. elegans* receptors are also not sensitive to nicotine. Of interest to our study is the *C. elegans* excitatory GABAR EXP-1, of which phylogenetic analysis suggests that it has evolved along an analogous, but opposite, evolutionary track (Fig. 6) (Beg and Jorgensen, 2003). In fact, most convertant LGICs, such as the *C. elegans* serotonin-gated (Ranganathan et al., 2000) *Drosophila melanogaster* histamine-gated chloride channels (Gisselmann et al., 2002, 2004) and the invertebrate inhibitory glutamate receptors (Cully et al., 1994, 1996; Horoszok et al., 2001), appear to originate from mutations in the LBD that induced changes in ligand specificity. This shows that mutations in either LBD or ion channel pore domains functionally contributed to LGIC subtype diversity in invertebrates. None of these receptor types, however, seem to have originated from recombination of LBD and ion channel domains.

Given the limited number of neurons, an increase in functional diversity of LGICs might serve to enhance the information handling capacity of the molluscan CNS. In molluscan species, fast synaptic chemical transmission of a single interneuron can have different effects (i.e., excitation, inhibition, or biphasic modulation) on the different postsynaptic partners (Wachtel and Kandel, 1971; Syed et al., 1990; Yeoman et al., 1993). Therefore, LGIC diversity in the invertebrate CNS might prevent the requirement for multiple interneurons, which each use a different transmitter type to impose opposite electrical polarization of follower neurons. As such, the demonstration of various invertebrate LGICs with mixed repertoires of selectivity for neurotransmitters versus cations or anions hints at fundamental differences between invertebrate and vertebrate nervous system evolution.

References

Alkondon M, Pereira EF, Wonnacott S, Albuquerque EX (1992) Blockade of nicotinic currents in hippocampal neurons defines methyllycaconitine as a potent and specific receptor antagonist. Mol Pharmacol 41:802–808.

Alkondon M, Pereira EF, Cortes WS, Maelicke A, Albuquerque EX (1997) Choline is a selective agonist of alpha7 nicotinic acetylcholine receptors in the rat brain neurons. Eur J Neurosci 9:2734–2742.

Barry PH (1994) JPCalc, a software package for calculating liquid junction potential corrections in patch-clamp, intracellular, epithelial and bilayer measurements and for correcting junction potential measurements. J Neurosci Methods 51:107–116.

Beg AA, Jorgensen EM (2003) EXP-1 is an excitatory GABA-gated cation channel. Nat Neurosci 6:1145–1152.

Benjamin PR, Elliott CJH (1989) Snail feeding oscillator: the central pattern generator and its control by modulatory interneurons. In: Neuronal and cellular oscillators (Jacklet JW, ed), pp 173–214. New York: Dekker.

Bertrand D, Ballivet M, Rungger D (1990) Activation and blocking of neuronal nicotinic acetylcholine receptor reconstituted in *Xenopus* oocytes. Proc Natl Acad Sci USA 87:1993–1997.

Bhandal NS, Ramsey RL, Harvey RJ, Darlison MG, Usherwood PN (1995) Channel gating in the absence of agonist by a homo-oligomeric molluscan GABA receptor expressed in *Xenopus* oocytes from a cloned cDNA. Invert Neurosci 1:267–272.

Bouzat C, Gumilar F, Spitzmaul G, Wang HL, Rayes D, Hansen SB, Taylor P, Sine SM (2004) Coupling of agonist binding to channel gating in an ACh-binding protein linked to an ion channel. Nature 430:896–900.

Buisson B, Bertrand D (2001) Chronic exposure to nicotine upregulates the human $\alpha 4\beta 2$ nicotinic acetylcholine receptor function. J Neurosci 21:1819–1829.

Chemeris NK, Kazachenko VN, Kislov AN, Kurchikov AL (1982) Inhibition of acetylcholine responses by intracellular calcium in *Lymnaea stagnalis* neurones. J Physiol (Lond) 323:1–19.

Chomczynski P, Sacchi N (1987) Single-step method of RNA isolation by acid guanidinium thiocyanate-phenol-chloroform extraction. Anal Biochem 162:156–159.

Corringer PJ, Bertrand S, Galzi JL, Devillers-Thiery A, Changeux JP, Bertrand D (1999) Mutational analysis of the charge selectivity filter of the alpha7 nicotinic acetylcholine receptor. Neuron 22:831–843.

Costa PF, Emilio MG, Fernandes PL, Ferreira HG, Ferreira KG (1989) Determination of ionic permeability coefficients of the plasma membrane of *Xenopus laevis* oocytes under voltage clamp. J Physiol (Lond) 413:199–211.

Couturier S, Bertrand D, Matter JM, Hernandez MC, Bertrand S, Millar N, Valera S, Barkas T, Ballivet M (1990) A neuronal nicotinic acetylcholine receptor subunit (alpha 7) is developmentally regulated and forms a homo-oligomeric channel blocked by alpha-BTX. Neuron 5:847–856.

Covernton PJ, Connolly JG (2000) Multiple components in the agonist concentration-response relationships of neuronal nicotinic acetylcholine receptors. J Neurosci Methods 96:63–70.

Cully DF, Vassilatis DK, Liu KK, Paress PS, Van der Ploeg LH, Schaeffer JM, Arena JP (1994) Cloning of an avermectin-sensitive glutamate-gated chloride channel from *Caenorhabditis elegans*. Nature 371:707–711.

Cully DF, Paress PS, Liu KK, Schaeffer JM, Arena JP (1996) Identification of a *Drosophila melanogaster* glutamate-gated chloride channel sensitive to the antiparasitic agent avermectin. J Biol Chem 271:20187–20191.

Davies PA, Wang W, Hales TG, Kirkness EF (2003) A novel class of ligand-gated ion channel is activated by Zn^{2+}. J Biol Chem 278:712–717.

Eisele JL, Bertrand S, Galzi JL, Devillers-Thiery A, Changeux JP, Bertrand D (1993) Chimaeric nicotinic-serotonergic receptor combines distinct ligand binding and channel specificities. Nature 366:479–483.

Elgoyhen AB, Johnson DS, Boulter J, Vetter DE, Heinemann S (1994) Alpha 9: an acetylcholine receptor with novel pharmacological properties expressed in rat cochlear hair cells. Cell 79:705–715.

Elgoyhen AB, Vetter DE, Katz E, Rothlin CV, Heinemann SF, Boulter J (2001) Alpha10: a determinant of nicotinic cholinergic receptor function in mammalian vestibular and cochlear mechanosensory hair cells. Proc Natl Acad Sci USA 98:3501–3506.

Galzi JL, Devillers-Thiery A, Hussy N, Bertrand S, Changeux JP, Bertrand D (1992) Mutations in the channel domain of a neuronal nicotinic receptor convert ion selectivity from cationic to anionic. Nature 359:500–505.

Gerzanich V, Anand R, Lindstrom J (1994) Homomers of alpha 8 and alpha 7 subunits of nicotinic receptors exhibit similar channel but contrasting binding site properties. Mol Pharmacol 45:212–220.

Gisselmann G, Pusch H, Hovemann BT, Hatt H (2002) Two cDNAs coding for histamine-gated ion channels in *D. melanogaster*. Nat Neurosci 5:11–12.

Gisselmann G, Plonka J, Pusch H, Hatt H (2004) Unusual functional properties of homo- and heteromultimeric histamine-gated chloride channels of *Drosophila melanogaster*: spontaneous currents and dual gating by GABA and histamine. Neurosci Lett 372:151–156.

Gunthorpe MJ, Lummis SC (2001) Conversion of the ion selectivity of the 5-HT(3a) receptor from cationic to anionic reveals a conserved feature of the ligand-gated ion channel superfamily. J Biol Chem 276:10977–10983.

Horoszok L, Raymond V, Sattelle DB, Wolstenholme AJ (2001) GLC-3: a novel fipronil and BIDN-sensitive, but picrotoxinin-insensitive, L-glutamate-gated chloride channel subunit from *Caenorhabditis elegans*. Br J Pharmacol 132:1247–1254.

Jensen ML, Timmermann DB, Johansen TH, Schousboe A, Varming T, Ahring PK (2002) The beta subunit determines the ion selectivity of the GABAA receptor. J Biol Chem 277:41438–41447.

Jensen ML, Schousboe A, Ahring PK (2005a) Charge selectivity of the Cys-loop family of ligand-gated ion channels. J Neurochem 92:217–225.

Jensen ML, Pedersen LN, Timmermann DB, Schousboe A, Ahring PK (2005b) Mutational studies using a cation-conducting GABAA receptor reveal the selectivity determinants of the Cys-loop family of ligand-gated ion channels. J Neurochem 92:962–972.

Johnson DS, Martinez J, Elgoyhen AB, Heinemann SF, McIntosh JM (1995) Alpha-conotoxin ImI exhibits subtype-specific nicotinic acetylcholine receptor blockade: preferential inhibition of homomeric alpha 7 and alpha 9 receptors. Mol Pharmacol 48:194–199.

Kehoe J (1972a) Ionic mechanisms of a two-component cholinergic inhibition in *Aplysia* neurones. J Physiol (Lond) 225:85–114.

Kehoe J (1972b) Three acetylcholine receptors in *Aplysia* neurones. J Physiol (Lond) 225:115–146.

Kehoe J, McIntosh JM (1998) Two distinct nicotinic receptors, one pharmacologically similar to the vertebrate $\alpha 7$-containing receptor, mediate Cl currents in *Aplysia* neurons. J Neurosci 18:8198–8213.

Kehoe J, Sealock R, Bon C (1976) Effects of alpha-toxins from *Bungarus multicinctus* and *Bungarus caeruleus* on cholinergic responses in *Aplysia* neurons. Brain Res 107:527–540.

Keramidas A, Moorhouse AJ, French CR, Schofield PR, Barry PH (2000) M2 pore mutations convert the glycine receptor channel from being anion- to cation-selective. Biophys J 79:247–259.

Keramidas A, Moorhouse AJ, Pierce KD, Schofield PR, Barry PH (2002) Cation-selective mutations in the M2 domain of the inhibitory glycine receptor channel reveal determinants of ion-charge selectivity. J Gen Physiol 119:393–410.

Keramidas A, Moorhouse AJ, Schofield PR, Barry PH (2004) Ligand-gated ion channels: mechanisms underlying ion selectivity. Prog Biophys Mol Biol 86:161–204.

Koert CE, Spencer GE, van Minnen J, Li KW, Geraerts WP, Syed NI, Smit AB, van Kesteren RE (2001) Functional implications of neurotransmitter expression during axonal regeneration: serotonin, but not peptides, autoregulate axon growth of an identified central neuron. J Neurosci 21:5597–5606.

Le Novere N, Changeux JP (1995) Molecular evolution of the nicotinic ace-

tylcholine receptor: an example of multigene family in excitable cells. J Mol Evol 40:155–172.

Orr-Urtreger A, Goldner FM, Saeki M, Lorenzo I, Goldberg L, De Biasi M, Dani JA, Patrick JW, Beaudet AL (1997) Mice deficient in the alpha7 neuronal nicotinic acetylcholine receptor lack alpha-bungarotoxin binding sites and hippocampal fast nicotinic currents. J Neurosci 17:9165–9171.

Ortells MO, Lunt GG (1995) Evolutionary history of the ligand-gated ion-channel superfamily of receptors. Trends Neurosci 18:121–127.

Palma E, Bertrand S, Binzoni T, Bertrand D (1996) Neuronal nicotinic alpha 7 receptor expressed in *Xenopus* oocytes presents five putative binding sites for methyllycaconitine. J Physiol 491:151–161.

Papke RL, Bencherif M, Lippiello P (1996) An evaluation of neuronal nicotinic acetylcholine receptor activation by quaternary nitrogen compounds indicates that choline is selective for the alpha 7 subtype. Neurosci Lett 213:201–204.

Putrenko I, Zakikhani M, Dent JA (2004) A family of acetylcholine-gated chloride channel subunits in *Caenorhabditis elegans*. J Biol Chem 280:6392–6398.

Ranganathan R, Cannon SC, Horvitz HR (2000) MOD-1 is a serotonin-gated chloride channel that modulates locomotory behaviour in *C. elegans*. Nature 408:470–475.

Schoepfer R, Conroy WG, Whiting P, Gore M, Lindstrom J (1990) Brain alpha-bungarotoxin binding protein cDNAs and MAbs reveal subtypes of this branch of the ligand-gated ion channel gene superfamily. Neuron 5:35–48.

Syed NI, Bulloch AG, Lukowiak K (1990) In vitro reconstruction of the respiratory central pattern generator of the mollusk *Lymnaea*. Science 250:282–285.

Tauc L, Gerschenfeld HM (1962) A cholinergic mechanism of inhibitory synaptic transmission in a molluscan nervous system. J Neurophysiol 25:236–262.

Thompson JD, Gibson TJ, Plewniak F, Jeanmougin F, Higgins DG (1997) The CLUSTAL_X windows interface: flexible strategies for multiple sequence alignment aided by quality analysis tools. Nucleic Acids Res 25:4876–4882.

Verbitsky M, Rothlin CV, Katz E, Elgoyhen AB (2000) Mixed nicotinic-muscarinic properties of the alpha9 nicotinic cholinergic receptor. Neuropharmacology 39:2515–2524.

Vulfius CA, Tumina OB, Kasheverov IE, Utkin YN, Tsetlin VI (2005) Diversity of nicotinic receptors mediating Cl(−) current in *Lymnaea* neurons distinguished with specific agonists and antagonist. Neurosci Lett 373:232–236.

Vulfius EA, Veprintzev BN, Zeimal EV, Michelson MJ (1967) Arrangement of cholinoreceptors on the neuronal membrane of two pulmonate gastropods. Nature 216:400–401.

Wachtel H, Kandel ER (1971) Conversion of synaptic excitation to inhibition at a dual chemical synapse. J Neurophysiol 34:56–68.

Ward JM, Cockcroft VB, Lunt GG, Smillie FS, Wonnacott S (1990) Methyllycaconitine: a selective probe for neuronal alpha-bungarotoxin binding sites. FEBS Lett 270:45–48.

Weber W (1999) Ion currents of *Xenopus laevis* oocytes: state of the art. Biochim Biophys Acta 1421:213–233.

Woodin MA, Munno DW, Syed NI (2002) Trophic factor-induced excitatory synaptogenesis involves postsynaptic modulation of nicotinic acetylcholine receptors. J Neurosci 22:505–514.

Wotring VE, Miller TS, Weiss DS (2003) Mutations at the GABA receptor selectivity filter: a possible role for effective charges. J Physiol (Lond) 548:527–540.

Yeoman MS, Parish DC, Benjamin PR (1993) A cholinergic modulatory interneuron in the feeding system of the snail, *Lymnaea*. J Neurophysiol 70:37–50.